Published in final edited form as:
Mech Dev. 2008 ; 125(3-4): 299–313. doi:10.1016/j.mod.2007.11.001.

Transcription factor broad suppresses precocious development of adult structures during larval–pupal metamorphosis in the red flour beetle, *Tribolium castaneum*

R. Parthasarathy, **A. Tan**, **H. Bai**, and **Subba R. Palli***
Department of Entomology, College of Agriculture, University of Kentucky, Lexington, KY 40546, United States

Abstract

Broad (br), a transcription factor containing the Broad-Tramtrack-Bric-a-brac (BTB) and zinc finger domains was shown to mediate 20-hydroxyecdysone (20E) action and pupal development in *Drosophila melanogaster* and *Manduca sexta*. We determined the key roles of br during larval–pupal metamorphosis using RNA interference (RNAi) in a coleopteran insect, *Tribolium castaneum*. Two major peaks of *T. castaneum* broad (Tcbr) mRNA, one peak at the end of feeding stage prior to the larvae entering the quiescent stage and another peak during the quiescent stage were detected in the whole body and midgut tissue dissected from staged insects. Expression of br during the final instar larval stage is essential for successful larval–pupal metamorphosis, because, RNAi-mediated knock-down of Tcbr during this stage derailed larval–pupal metamorphosis and produced insects that showed larval, pupal and adult structures. Tcbr dsRNA injected into the final instar larvae caused reduction in the mRNA levels of genes known to be involved in 20E action (EcRA, E74 and E75B). Tcbr dsRNA injected into the final instar larvae also caused an increase in the mRNA levels of JH-response genes (JHE and Kr-h1b). Knock-down of Tcbr expression also affected 20E-mediated remodeling of midgut during larval–pupal metamorphosis. These data suggest that the expression of Tcbr during the final instar larval stage promotes pupal program while suppressing the larval and adult programs ensuring a transitory pupal stage in holometabolous insects.

Keywords

RNAi; Metamorphosis; Gene expression; BTB-POZ domain; Ecdysone; Juvenile hormone

1. Introduction

Metamorphosis in holometabolous insects ensures transformation of larva into a reproductive adult through a transitory pupal stage. A complex series of developmental events involving programmed cell death, cell proliferation and differentiation and remodeling of structures occur during metamorphosis. These events are regulated by the changing titers of 20-hydroxyecdysone (20E) and juvenile hormone (JH) (Riddiford, 1994, 1996). The hormonal regulation of metamorphosis has been studied extensively in *Drosophila melanogaster* (Ashburner, 1970; Postlethwait, 1974; Riddiford and Ashburner, 1991; Restifo and Wilson, 1998), *Manduca sexta* (Riddiford, 1976, 1978; Zhou et al., 1998; Zhou and Riddiford, 2001, 2002) and *Bombyx mori* (Reza et al., 2004).

*Corresponding author: Tel.: +1 859 257 4962; fax: +1 859 323 1120. rpalli@email.uky.edu (S.R. Palli).

A small rise in 20E levels during the final instar larval stage terminates larval feeding, initiates premetamorphic behavior, and commits the animal to a pupal fate (Nijhout, 1994). This commitment peak of 20E activates and coordinates expression of a cascade of genes including a number of transcription factors (Russell and Ashburner, 1996; Thummel, 1996). Broad (br) is one of the 20E-induced early genes and a transcription factor containing the Broad-Tramtrack-Bric-a-brac (BTB) and zinc finger domains (Zollman et al., 1994). Broad plays critical roles in metamorphosis of *D. melanogaster* where its null mutant *non-pupariating* failed to undergo larval–pupal transformation (Kiss et al., 1976, 1988). Broad expression has been projected as one of the first molecular events underlying pupal commitment in *M. sexta* (Zhou et al., 1998; Zhou and Riddiford, 2001) and the control of br expression by JH has been addressed in the epidermis of the above two insects during the pupal–adult molt (Zhou and Riddiford, 2002). From the above studies it is clear that br is expressed specifically during larval–pupal metamorphosis under the control of 20E and JH. The role of br in metamorphosis of *B. mori* has been demonstrated using RNA interference (RNAi) experiments (Uhlirova et al., 2003). However, the effects of RNAi have been observed only during the pupal stage in *B. mori* as opposed to the effects observed during prepupal stage of br mutants in *D. melanogaster* (Kiss et al., 1988). This might be due to the delay in virus-mediated RNAi effect in *B. mori*. In hemimetabolous insect, milkweed bug, *Oncopeltus fasciatus*, br was shown to be necessary for the heteromorphic changes that occur during development (Erezyilmaz et al., 2006).

In this study, we determined the role of br during larval–pupal metamorphosis using RNAi in *Tribolium castaneum*. *T. castaneum* is an ideal model insect to perform these studies because of functioning of systemic RNAi. Moreover, it evokes additional interest as patterning of most of the imaginal structures occurs at the end of the larval stage (Quennedey and Quennedey, 1990; Tower, 1903; Nagel, 1934) unlike in other insects (Svacha, 1992). Here, we demonstrate the conserved role of *T. castaneum* broad (Tcbr) in specifying pupal stage in *T. castaneum*. Additionally, we provide evidence that Tcbr promotes pupal development by suppressing precocious adult development during larval–pupal metamorphosis.

2. Results

2.1. Ecdysteroid titers in T. castaneum

Ecdysteroid titers were determined during the final instar larval and pupal stages (Fig. 1). The ecdysteroid levels were low during the final instar larval stage except for small increases at 60, 78 and 90 h after ecdysis into the final instar larval stage (AEFL, Fig. 1A). The ecdysteroid titers began to increase at the beginning of quiescent stage and reached the maximum levels by the end of the quiescent stage prior to pupation. The ecdysteroid titers were low at the beginning of the pupal stage and increased again starting at 42 h after ecdysis into the pupal stage (AEPS) and reached the maximum levels by 66 h AEPS (Fig. 1B). Then the ecdysteroid levels decreased and reached the minimum levels prior to adult emergence at 96 h AEPS.

2.2. Developmental changes in Tcbr mRNA

The mRNA levels of Tcbr were determined in the whole body as well as in the midgut tissue collected at 12 h intervals during the final instar larval and pupal stages (Fig. 2). Four isoforms of Tcbr that contain common BTB domain and variable number of zinc fingers are present in the genome of *T. castaneum* (GenBank Gene ID 659193 contains 15,532 bp sequence and specific exons for all four isoforms). In this study, we used primers designed based on the sequence in the common region of Tcbr; therefore, these primers detect all four isoforms. In the whole body samples, the mRNA levels of Tcbr were low during the early

stages of last instar larval stage. The Tcbr mRNA levels increased beginning at 48 h AEFL and reached the maximum by 84 h AEFL. Then the Tcbr mRNA levels decreased and reached the minimum by the end of the feeding stage (96 h AEFL) prior to the larvae entering the quiescent stage. The Tcbr mRNA levels increased again beginning at 0 h after the larvae entering into the quiescent stage and continued to increase until pupal ecdysis. The Tcbr mRNA levels suddenly declined at 12 h after pupal ecdysis and the Tcbr mRNA levels remained low during the rest of the pupal stage. The Tcbr mRNA levels in the midgut increased beginning at 24 h AEFL and reached the maximum by 84 h AEFL. Then the Tcbr mRNA levels in the midgut began to decrease and reached the minimum by the end of the feeding stage (96 h AEFL). The Tcbr mRNA levels in the midgut increased again beginning at 12 h after the larvae entering into the quiescent stage and reached the maximum by 24 h after the larvae entering into the quiescent stage. The Tcbr mRNA levels suddenly declined soon before pupal ecdysis and the Tcbr mRNA levels remained low during the rest of the pupal stage (Fig. 2).

2.3. Tcbr RNAi affects the expression of 20E- and JH-response genes

To determine the effectiveness of dsRNA in knock-down of Tcbr, the Tcbr mRNA levels were quantified in dsRNA injected insects and control insects that were injected with dsRNA prepared using *malE* of *Escherichia coli* as a template (Fig. 3). The larvae injected during the penultimate stage were sampled at 5 days after injection (=72 h AEFL, Fig. 3a). The larvae injected at 24 h AEFL were sampled at 5 days after injection (=36 h after the larvae entered the quiescent stage, Fig. 3b). The larvae injected at 72 h AEFL were sampled at 4 days after injection (=24 h AEPS, Fig. 3c). The mRNA levels of Tcbr were reduced by 2- to 4-fold in insects injected with Tcbr dsRNA when compared to its mRNA levels in *malE* dsRNA injected control insects (Fig. 3).

To determine the effect of knock-down of Tcbr on the expression of 20E- and JH-response genes, mRNA levels of these genes were compared in the total RNA isolated from insects injected with Tcbr or *malE* dsRNA (control). In the insects injected with Tcbr dsRNA, mRNA levels of Tcbr and other 20E-induced genes, EcRA, E74 and E75B were 1.5- to 2-fold less when compared to their mRNA levels in the control (Fig. 4). The expression of other genes involved in 20E action, EcRB, HR3, FTZ-F1 and E75A was unaffected by Tcbr knock-down. Also, JH-response genes, JHE and Kr-h1B were 3- and 4-fold higher in insects injected with Tcbr dsRNA when compared to their mRNA levels in control insects injected with *malE* dsRNA (Fig. 4). These data showed that Tcbr may be involved in regulating the expression of some 20E- (EcRA, E74 and E75B) and JH-response genes.

2.4. Tcbr knock-down derails larval–pupal metamorphosis

To determine the role of Tcbr in metamorphosis, the dsRNA prepared using the common region of Tcbr as a template was injected into the penultimate and final instar larvae. The control larvae were injected with *malE* dsRNA. Knock-down in Tcbr expression resulted in a block in metamorphosis (Table 2). When injected into the penultimate instar larvae, all the insects successfully molted into the next larval stage but did not develop into pupae as they died during the next molt. 28 out of 30 larvae injected with Tcbr dsRNA at 24 h AEFL died due to unsuccessful molt to the next stage and showed larval–pupal and adult characters. When Tcbr dsRNA was injected at 72 h AEFL, 25 out of 30 Tcbr dsRNA injected insects completed the next molt but the molted insects showed larval–pupal–adult structures and died soon after molting. Most of the control insects (except for a few that died during the first two days after injection most likely due to injury from injection) injected with *malE* dsRNA developed normally and emerged as adults (Table 2).

The penultimate larvae injected with Tcbr dsRNA molted into the next larval stage and progressed to the next molt but did not complete ecdysis during this molt. A dorsal split on the thorax was observed indicating the initiation of ecdysis but the ecdysis was not completed (Fig. 5a, blue arrow). These insects showed the development of compound eyes (Fig. 5b, red arrowhead), differentiated legs (green arrow) and wing pads (white star) and died during this stage. When Tcbr dsRNA was injected at 24 h AEFL, the molt into the next stage was incomplete and the exuviae remained attached to the body (Figs. 5c and d, blue arrow). When the exuviae was physically removed, these insects showed larval (abdominal cuticle and distal segments), pupal (compound eyes, genital papillae, urogomphi) and adult (antennae, legs, wings) structures. When the Tcbr dsRNA was injected at 72 h AEFL, the insects molted into the next stage but these insects also showed larval–pupal–adult intermediate characters as above and died during this stage. In both cases, antennae (Figs. 5c and e, black arrow) and legs (Figs. 5d and f, green arrow) were well differentiated; wings (Figs. 5c and e, white arrow) were sclerotized at the margins similar to the structures in the pharate adults rather than in the pupa. Control larvae for all the treatments successfully pupated (Figs. 5g and h) and the pupal cuticle possessed a distinguishing structure called gin-traps (Figs. 5g, black star). Gin-traps, a pupal character were absent in insects developed from final instar larvae injected with Tcbr dsRNA. Thus, knock-down of expression of Tcbr during the final instar larval stage produced insects that showed larval, pupal and adult characters and failed to develop further and died.

The abnormal phenotypes caused by Tcbr dsRNA injection were analyzed further by SEM. The depletion of Tcbr mRNA affected multiple tissues. The thoracic sternal plates supporting the legs were not prominent in the larval stages (Fig. 6a). These plates develop at the end of the pupal stage (Fig. 6b) and become distinct and sclerotized in the adults (Fig. 6c). Tcbr dsRNA injected insects showed distinct thoracic sternal sclerites (Fig. 6d) similar to those seen in the adults. Larval antennae show simple structure containing only two segments, scape and pedicel (Fig. 6e). The flagellar segments are formed during the pupal stage (Fig. 6f). The flagellae differentiate into multi-segmented structures at the end of the pupal stage and develop into fully functional adult antennae containing hygroscopic receptors (Fig. 6g). Depletion of Tcbr in the final instar larvae resulted in the precocious formation of flagellar segments in the antennae but the complete differentiation and formation of hygroscopic receptors were lacking (Fig. 6h). The mouthparts of larvae are represented by well developed mandibles. The maxillary and labial palpi are small and the labrum is concealed (Fig. 6i). During the pupal stage, the labrum becomes well developed and hence the mandibles look separated. The maxillary and labial palpi start differentiating into distinct structures (Fig. 6j). In the adults, the mandibles appear to be interlocked with their incisors at the tip remain overlapped. The maxillary and labial palpi are well developed (Fig. 6k). Insects injected with Tcbr dsRNA developed mouthparts that showed pupal and adult structures. The labrum was well developed and the maxillary and labial palpi were distinct similar to those seen in pupae. However, there was no gap between the incisors of mandibles as observed in the pupal stage and they appeared to be interlocked as seen in adults (Fig. 6l).

During the final instar larval stage of *T. castaneum*, epidermal cells in the lateral margins of the meso- and metathorax become columnar and proliferate to form wings (Quennedey and Quennedey, 1990). Larvae contain no wings (Fig. 7a) and the wings are formed during the larval–pupal metamorphosis and cover two-third of the abdomen of the pupa (Fig. 7b). Sclerotization of the forewings occurs in the pharate adult; the elytra are completely developed covering the hindwings (Fig. 7c). Knocking-down Tcbr during the final instar larval stage resulted in the malformation of wings. Both forewings and hindwings were short and because of under development of wings, the hindwings were exposed unlike in adults (Fig. 7d).

Prothetely is observed in larval legs of *T. castaneum* (Nagel, 1934) wherein the portions representing the future adult legs are seen. The larval legs possess a single claw at the end (Fig. 7e). During the pupal stage, the legs remain enclosed within pupal cuticle and elongation of femur and tibia, and differentiation of tarsal segments occur (Fig. 7f). In the adults, the distinct segments of legs such as coxa, trochanter, femur, tibia and tarsi are seen with formation of spurs. The distal tarsal segment bears two claws (Fig. 7g). The depletion of Tcbr during the final instar larval stage caused development of legs that showed adult characters. Distinct tarsal segments terminating in two claws were observed. The elongation of femur and tibia were incomplete. Though short, the legs of insects injected with Tcbr dsRNA looked similar to adult legs rather than larval and pupal legs (Fig. 7h).

The cuticular processes/appendages are distinct in larval/pupal and adult stages of *T. castaneum*. The larval abdominal cuticle bears bunches of long setae (Fig. 7i). The pupal abdominal cuticle has distinct structures called gin-traps on the lateral sides of the abdomen and the pupal cuticular appendages are shorter than the larval counterparts and bear a distinct articulating membrane at their bases (Fig. 7j). In the case of adults, the abdominal cuticle bears sensory bristles (Fig. 7k). In Tcbr dsRNA injected insects, the abdominal cuticle was a mosaic with the presence of long setae typical to larval cuticle and patches of sensory bristles as seen in adult cuticle (Fig. 7l).

The development of male genitalia in dsRNA injected insects was similar to that observed in pupa (Figs. 8b and c) while the development of female genitalia was incomplete when compared to pupal counterpart (Figs. 8e and f). The larval pygopods (Fig. 8a) were absent in the Tcbr dsRNA injected insects. The urogomphi in the injected insects was similar to that of pupal urogomphi rather than larval urogomphi in structure, but resembled larval urogomphi with respect to sclerotization (see Figs. 5e and f). The larval urogomphi is distinct with a median connecting both at the top (Fig. 8a). The distal segment of the abdomen is shortened in both male and female pupa (Figs. 8b and e) and is telescopic in adults (Fig. 8d), whereas in Tcbr dsRNA injected insects the distal abdominal segments looked like larval counterparts (Figs. 8c and f). The phenotypes caused by Tcbr RNAi in comparison with larval, pupal and adult structures are summarized in Table 3.

2.5. Tcbr is required for midgut remodeling

Our expression analysis of Tcbr in the midgut indicated the possible roles for Tcbr in the midgut remodeling as the increase in Tcbr mRNA levels coincided with the timing of midgut remodeling during the larval–pupal metamorphosis. Hence, cross-sections of midguts from insects injected with Tcbr dsRNA showing knock-down phenotypes and their control counterparts were nuclear stained with DAPI (Fig. 9). The midguts dissected from the control insects that were at pupal stage showed formation of pupal midgut epithelium as the larval cells moved into the lumen (Fig. 9a). The midgut dissected from insects injected with Tcbr dsRNA at 24 h AEFL consisted of mostly larval cells (large nuclei) and a few stem cells (small nuclei) and the larval cells remained attached to the epithelium (Fig. 9b). The midguts dissected from the insects injected with Tcbr dsRNA at 72 h AEFL were at advanced stage of remodeling when compared to the midguts dissected from the control insects (Fig. 9c). Evagination of crypts (Fig. 9d, marked with star), a distinguishing character of adult midgut that occurs during the pharate adult stage was observed in these midguts indicating that knock-down of Tcbr at 72 h AEFL did not block midgut remodeling but adult midgut characters were expressed in the larva–pupa–adult intermediate insects.

Since the initial analysis showed that the knock-down of Tcbr may affect midgut remodeling by blocking the division of stem cells, cell proliferation assay was performed by BrdU labeling. The insects were administered with BrdU at four days after injection of dsRNA and the midguts were dissected and stained to detect BrdU (Fig. 10). The midgut of insects

injected with Tcbr dsRNA at 24 h AEFL showed a very few BrdU positive cells (Figs. 10a–c) when compared to the midguts dissected from control insects (Figs. 10d–f) indicating a block in cell proliferation. Midgut of insects injected with Tcbr dsRNA at 72 h AEFL showed extensive proliferation of cells only in the evaginated regions (crypts), but not in the cells constituting the pupal gut epithelium (Figs. 10g–i). In the control insects that already developed into pupae showed concentric rings of proliferative cells which were about to evaginate. Also, most of the pupal gut epithelial cells were still proliferative (Figs. 10j–l).

To assess the effect of silencing of Tcbr on the hormonal regulation of cell proliferation in the midguts, *in vitro* assays and BrdU labeling were performed. dsRNA for Tcbr or *malE* was injected at 24 h AEFL. Midguts dissected at two days after injection were cultured *in vitro* for two additional days. During the incubation, the midguts were exposed to 10 μM 20E, 10 μM JH III or 10 μM each of 20E and JH III for 24 h. BrdU pulsing was done for 12 h followed by BrdU labeling and detection. Relative fluorescent intensity (RFI) of BrdU positive cells was measured in midguts. In control midguts, 20E induced cell proliferation (Fig. 11). DMSO and JH III alone did not show any effect on cell proliferation. However, addition of JH III to 20E reduced 20E-induced cell proliferation by 50%. Knock-down of Tcbr mRNA reduced 20E-induced cell proliferation by almost 3-fold suggesting that Tcbr is required for 20E mediated cell proliferation. In the midguts isolated from larvae injected with Tcbr dsRNA, addition of JH III alone or in combination with 20E reduced cell proliferation suggesting that Tcbr is not required for JH action on 20E induced cell proliferation.

3. Discussion

The metamorphosis in holometabolous insects is regulated by changing titers of ecdysteroids and JH. A small peak of ecdysteroids in the absence of JH (commitment peak) during the final instar larval stage induces pre-metamorphic behavior. A large peak of ecdysteroids during the prepupal stage induces pupation. The peak of ecdysteroids detected during the quiescent stage prior to pupation in *T. castaneum* is most likely similar to the prepupal peak reported for other insects (Riddiford, 1993, 1994; Margam et al., 2006). Rise in ecdysteroid levels were observed at 60, 78 and 90 h AEFL also. One of these increases in ecdysteroids in the absence of JH probably commits *T. castaneum* larvae to pupal program. Pre-liminary determination of JH titers in *T. castaneum* showed higher JH III levels at the beginning of the final instar larval stage and decreased at the end of feeding period but increased again resulting in a large peak of JH during the quiescent stage (data not shown). Juvenile hormone analog, hydroprene sensitivity to *T. castaneum* decreased after 72 h AEFL suggesting that these larvae may commit to pupal program prior to 72 h AEFL (Parthasarathy and Palli, unpublished). Interestingly, the expression of Tcbr mRNA levels in the whole body increased at 60 h AEFL and reached the maximum levels by 84 h. The ecdysteroid rise at 60 h AEFL probably induces the expression of Tcbr. This is in agreement with the findings in *Drosophila* that Broad proteins were present in several tissues such as salivary gland, gut, fat body, wing imaginal disc and central nervous system before the major pulse of ecdysone in the late third instar and their concentrations increased after the ecdysone pulse (Emery et al., 1994). Taken together these data suggest that the ecdysteroid rise at 60 h AEFL may be involved in commitment of *T. castaneum* larvae to pupal program.

Broad-complex (BR-C) has been most extensively characterized by classical genetics studies in *Drosophila*. The BR-C is defined by at least three lethal complementation groups: *br*, *rbp* and *l(l)2Bc* and mutations in each of these classes complement one another (Belyaeva et al., 1982; Kiss et al., 1988). Each of the BR-C functions defined by these three complementation groups were required for distinct aspects of imaginal disc morphogenesis during prepupal development (Fristrom et al., 1981; Kiss et al., 1988), complete

metamorphosis of the salivary gland, fat body, gut and dorsal flight muscles (Kiss et al., 1978; Fristrom et al., 1981; Restifo and White, 1992) and proper remodeling of the CNS (Restifo and White, 1991). Thus, studies using BR-C mutants of *D. melanogaster* (Kiss et al., 1988; Karim et al., 1993; Bayer et al., 1997), misexpression of br with JHA application in *M. sexta* (Zhou and Riddiford, 2002), and virus-mediated br RNAi knock-down in *B. mori* (Uhlirova et al., 2003) showed that br is a pupal specifier gene. Our studies in *T. castaneum* showed that pupal specifying function of Tcbr is conserved in this insect belonging to order Coleoptera.

RNAi studies in *T. castaneum* reported here suggest an additional role for Tcbr in suppression of development of adult structures during larval–pupal metamorphosis. Critical observation of individual tissues from Tcbr RNAi insects supports the above hypothesis based on the following observations: (1) silencing of Tcbr leads to synthesis of adult cuticle in the larval–pupal–adult intermediates as we observed mosaic of larval and adult cuticle in Tcbr RNAi insects. (2) Precocious development of adult characters was more pronounced in some organs. For example, the antennae of insects injected with Tcbr dsRNA had 10–11 flagellar segments similar to the adult antennae. The pupal antennae have only 4–5 flagellar segments and the remaining segments are formed at the end of the pupal stage. The structure and sclerotization of mandibles in Tcbr RNAi insects resembled adult mandibles rather than pupal mandibles. Also, the thoracic sternal plates were well developed in insects injected with Tcbr dsRNA and these structures were similar to those in adults. The abdominal cuticle of Tcbr RNAi insects had patches of adult cuticular structures. (3) Unlike the above organs, the differentiation of compound eyes, legs and wings were impaired by knocking-down Tcbr mRNA levels in the final instar larvae. Similar conditions were observed in br mutants of *D. melanogaster* (Kiss et al., 1988) and *B. mori* RNAi insects (Uhlirova et al., 2003). Particularly, in *Drosophila*, BR-C mutants prevented the morphogenesis of imaginal discs; mutations in br domain resulted in malformed wings and legs; wings were short and severely broad; legs were short, bulbous and often exhibited twisted segments (Kiss et al., 1988). In the present study, Tcbr RNAi insects showed short and broad wings; short, bulbous and undifferentiated legs. In general, the adult structures were at various stages of differentiation state. This condition may have arisen as prothetely is observed in *T. castaneum* larvae (Truman and Riddiford, 2002) and patterning of most of the imaginal structures occurs at the end of the larval stage (Quennedey and Quennedey, 1990; Tower, 1903; Nagel, 1934) unlike in other insects (Svacha, 1992). The Tcbr dsRNA injected insects resembled pharate adults rather than pupae. Thus, reduction in Tcbr mRNA levels during the final instar larval stage blocked pupal program and allowed development of adult structures in multiple tissues resulting in formation of larval–pupal–adult intermediates. Two factors may have contributed to the formation of larval–pupal–adult intermediates. Firstly, due to the difference in the timing of commitment and differentiation among pupal and adult structures, the development of some of these structures may have been initiated and progressed prior to silencing of Tcbr gene through RNAi. Secondly, the efficiency in silencing of Tcbr gene probably varied among various tissues leading to differential response of these tissues resulting in complete to partial block in some pupal structures (e.g. cuticle) to almost no effect on other structures (e.g. genital papillae).

In this study we also identified genes whose expression requires the presence of Tcbr. Expression of 20E-induced genes EcRA, E74 and E75 was down-regulated in Tcbr RNAi insects suggesting that Tcbr is required for complete expression of these genes. This is in accordance with the studies using Tcbr mutants of *D. melanogaster* wherein the expression of E74 and E75 was delayed or reduced (Guay and Guild, 1991; Karim et al., 1993). JHE is induced by juvenile hormone in *Choristoneura fumiferana* (Feng et al., 1999) and *D. melanogaster* (Kethidi et al., 2005). In *D. melanogaster* Kr-h1 is induced by 20E and EcR is required for 20E induction of this gene (Beckstead et al., 2005). In *D. melanogaster* L57

cells, Kr-h1 is induced by JH III (Palli, unpublished). In *T. castaneum* JHE is induced by JH III and Met is required for normal expression of both JHE and Kr-h1B (Tan and Palli, unpublished). Interestingly, in Tcbr RNAi insects, JHE and Kr-h1B mRNA levels were high when compared to the levels in control insects. In *M. sexta*, JH reappears during the prepupal peak of ecdysone regulating normal larval–pupal transition by preventing precocious adult development (Baker et al., 1987; Truman and Riddiford, 2002). It is likely that Broad RNAi insects maintain high JHE levels to prevent this JH action and promote precocious adult development. Further experiments are needed to characterize the role of Kr-h1B during larval–pupal metamorphosis.

Besides affecting the epidermal and cuticular structures, Tcbr RNAi also affected the remodeling of internal tissue, midgut. Midgut remodeling in *T. castaneum* begins at 96 h AEFL (Parthasarathy and Palli, unpublished) following the peaks of ecdysteroids (60, 78 and 90 h AEFL) and with the peak of Tcbr mRNA in the midgut (84 h AEFL). When injections of dsRNA for Tcbr were performed at 24 h AEFL, midgut remodeling was blocked, while injections of dsRNA at 72 h AEFL did not block midgut remodeling; but evagination of crypts, a characteristic feature of adult midgut was observed in these midguts. These data provide further evidence and confirm our conclusions that expression of Tcbr during the final instar larval stage is involved in reduction of differentiation of adult structures. JH reduction of 20E induction of stem cell proliferation was not affected by Tcbr knock-down suggesting that Tcbr is not involved in JH action in midgut. However, Tcbr RNAi insects showed increased expression of JH-response genes such as JHE and Kr-h1B in the whole body. Further investigations on the regulation of Tcbr and its downstream target genes in different tissues by JH are warranting. Taken together, we demonstrate that Tcbr, besides promoting pupal programming, is involved in the prevention of precocious development of adult structures during the larval–pupal metamorphosis, thus taking the insect through the transitory pupal stage.

4. Materials and methods

4.1. Rearing and staging

Strain GA-1 of *T. castaneum* (Haliscak and Beeman, 1983) was reared on organic wheat flour containing 10% yeast at 30 °C under standard conditions (Beeman and Staurt, 1990). Precise staging was done from the final instar larvae to adults closely following methods described in Arakane et al. (2005). The final instar larvae were identified as soon as they molted using untanned white cuticle as a marker and designated as 0 h AEFL. The larvae were staged from that time onwards. The beginning of quiescent stage was designated as 0 h and was determined based on cessation of feeding and movement. The following days in quiescent stage were recognized by characteristic ‘C’ shaped larvae. White pupae were designated as 0 h AEPS and staged thereafter. Formation of compound eyes at 48 AEPS, sclerotization of mandibles and forewings at 72 h AEPS, and pharate adults at 96 h AEPS were used as morphological characters for staging pupae. Adult eclosion occurs at four days after pupation.

4.2. Determination of ecdysteroid levels

For determination of ecdysteroid titer, staged insects were washed thoroughly in double distilled water and dried. The insects were homogenized in 250 μl of ice-cold 75% aqueous methanol and centrifuged at 13,000*g* at 4 °C. Supernatants were transferred to 6 × 50 mm borosilicate glass tubes; precipitates were resuspended in an additional 100 μl of aqueous methanol and kept on ice for 30 min. After centrifugation as above, the precipitates were vacuum dried. An enzyme immunoassay (EIA) was used to estimate ecdysteroid titers as previously described (Kingan and Adams, 2000; Gelman et al., 2002). The ecdysteroid anti-

serum used in the EIA has a high affinity for ecdysone (E), 20E, makisterone A, 20,26-dihydroxyecdysone, 26-hydroxyecdysone and 3-dehydroecdysone (Kingan, 1989, T.G. Kingan, personal communication), but does not detect polar conjugates (Gelman et al., 2005).

4.3. Double-stranded RNA (dsRNA) synthesis and injection

dsRNA of Tcbr-common region of *T. castaneum* was synthesized using the Ambion MEGAscript transcription kit (Ambion, Austin, TX). Cognate primers designed based on the sequence available in the Beetlebase (Table 1) containing T7 polymerase promoter sequence at their 5′ ends were used to amplify 150 bp common region of Tcbr. The resultant PCR product was used for transcription reaction as per the instruction manual. dsRNA was injected into the larvae on the dorsal side of the first or second abdominal segments using a aspirator tube assembly (Sigma) fitted with 3.5″ glass capillary tube (Drummond) pulled by a needle puller (Model P-2000, Sutter Instruments Co.). Approximately, 50 ng of dsRNA was injected per larva. Injected larvae were reared under standard conditions until use. Control larvae were injected with dsRNA for *E. coli malE* gene.

4.4. cDNA synthesis and quantitative real-time reverse-transcriptase PCR (qRT-PCR)

Total RNA was extracted from the whole body or midguts dissected from staged larvae and pupae using TRI reagent (Molecular Research Center Inc., Cincinnati, OH). cDNA was synthesized using 2 μg of DNAse1 (Ambion, Austin, TX) – treated RNA and iScript cDNA synthesis kit (Biorad Laboratories, Hercules, CA) in a 20 μl reaction volume as per the manufacturer's instructions. Real-time quantitative reverse-transcriptase PCR was performed using MyiQ single color real-time PCR detection system (Biorad Laboratories). PCR components were:1 μl of cDNA, 1 μl each of 10 μM forward and reverse sequence specific primers (Table 1), 7 μl of H_2O and 10 μl of supermix (Biorad Laboratories). PCR conditions were: 95 °C for 3 min followed by 45 cycles of 95 °C for 10 s, 60 °C for 20 s and 72 °C for 30 s. Both the PCR efficiency and R^2 (correlation coefficient) values were taken into account prior to estimating the relative quantities. Relative expression levels of each gene were quantified using ribosomal protein, rp49 expression levels as an internal control.

4.5. BrdU labeling and preparation of tissue sections

Staged larvae/pupae were injected with 0.1 μl of 10mM BrdU (Roche, Indianapolis, IN) into the haemocoel as described above. After 12 h, the midguts from injected insects were dissected. The sections were processed using 5-bromo-2′-deoxy-uridine Labeling and Detection kit I (Roche) according to manufacturer's instructions. The tissues were incubated with Texas-Red conjugated goat anti-mouse antibody (Molecular Probes) at 1:1000 dilutions. Controls included were midguts from insects that were not injected and midguts that were not exposed to anti-BrdU. After washing extensively in 1× PBS, the tissues were counterstained with DAPI and mounted with 50% glycerol in 1× PBS.

For preparation of tissue sections, the midguts from larvae and pupae injected with dsRNA for specific genes were dissected in 1× PBS (phosphate buffered saline, Sigma) and fixed in 4% paraformaldehyde (Sigma). Embedding and sectioning was done as previously described (Parthasarathy and Palli, 2007). The sections were deparaffinized through successive baths of Xylene, rehydrated through serial grades of ethanol, water and 1× PBS. Nuclear staining was done with DAPI (4′,6-Diamidino-2-phenyl indole, Sigma) at 1 μg/ml concentration for 10 min. The slides were washed with 1× PBS twice and mounted in 50% glycerol.

4.6. In vitro assays

The midguts dissected under aseptic conditions were cultured in Ex-Cell 420 Insect serum free medium (JRH Biosciences) containing the following antibiotics: antibiotic – antimycotic solution, 1× dilution (Sigma); Gentamicin solution, 200 μg/ml (Sigma); Penicillin–Streptomycin, 20 U/ml (Life Technologies) for 24 h at 27 °C. The entire medium was replaced with fresh medium containing appropriate concentrations of ligands (20E and JHIII, Sigma) and incubated for further 24 h. For BrdU incorporation, the midguts were pulsed with BrdU labeling reagent (Roche) at 1:1000 dilutions (final concentration 10 μM) for 12 h during this 24 h incubation period. The midguts were washed with 1× PBS and fixed in 4% paraformaldehyde for 1 h at room temperature. Then the tissues were processed for BrdU detection as described above.

4.7. Imaging and documentation

For light microscopy, the modular zoom system (Leica Z16 APO, Germany) fitted with JVC 3CCD Digital Camera KY-F75U was used. The images were documented using Cartograph version 6.1.0 (GT Vision Demonstration). Image processing was done using Archimed version 5.2.2 (Micovision Instruments).

For scanning electron microscopy, the insects were washed thoroughly in double distilled water thrice and then briefly in 0.1% Triton X-100 detergent solution to get rid of flour adhering to the insect. The insects were processed according to Nation (1983). Briefly, the insects were slowly dehydrated in series of ethanol (25%, 50%, 75%, 90% and 100%) by incubating in each concentration for 1 h with shaking. The insects were then immersed in HDMS (1,1,1,3,3,3 hexadimethyldisilazane) for 5 min., and air dried at room temperature. The insects were mounted on stainless steel stubs with sticky tape (RPI) under dust free conditions. The insects were then sputtered with gold using Hummer VI Sputtering System (Technics) at plasma discharge rate of 10 milliamperes for 180 s. Scans were performed with a Hitachi S-800 Scanning Electron Microscope at 10 kV and 10 milliamperes. Images were documented using Evex Nanoanalysis and Digital Imaging software (Evex Analytical version 2.0.1192).

For fluorescent images, an Olympus FV1000 laser scanning confocal microscope was used. DAPI and RFP were excited using 405 nm and 543 nm laser lines, respectively. When using multiple flours simultaneously, images were acquired sequentially, line-by-line, in order to reduce excitation and emission cross talk. The primary objective used was an Olympus water immersion PLAPO40XWLSM-NA1.0. Image acquisition was conducted at a resolution of 512 × 512 pixels and a scan-rate of 10 ms/pixel. Control of the microscope, as well as image acquisition and exportation as TIFF files, was conducted using Olympus Fluoview software version 1.5. Exposure settings that minimized oversaturated pixels in the final images were used. Optical sectioning was done and a composite *Z*-stack image was used, wherever necessary. Figures of all micrographs were assembled using Photoshop 7.0.

4.8. Statistical analysi1s

Analysis of variance was performed using SAS version 9.0 software (SAS Institute Inc., Cary, NC, USA). to test for statistical differences among treatments ($\alpha = 0.05$). Pairwise comparisons were made using the protected least squares difference (LSD) method.

Acknowledgments

This work was supported by National Science Foundation (IBN-0421856), National Institute of Health (GM070559-02) and National Research Initiative of the USDA-CSREES (2004-03070). We thank Drs. Michael Goodin, Sheryn Perry and Michael Sharkey and Mr. Dicky Yu for their help in histology and microscopic facilities.

We thank Dr. Dale B. Gelman from USDA, ARS, BARC for help with ecdysteroid determination. This is contribution number 07-08-130 from the Kentucky Agricultural Experimental Station.

References

Arakane Y, Muthukrishnan S, Kramer KJ, Specht CA, Tomoyasu Y, Lorenzen MD, Kanost M, Beeman RW. The Tribolium chitin synthase genes TcCHS1 and TcCHS2 are specialized for synthesis of epidermal cuticle and midgut peritrophic matrix. Insect Mol Biol. 2005; 14:453–463. [PubMed: 16164601]

Ashburner M. Effects of juvenile hormone on adult differentiation of *Drosophila melanogaster*. Nature. 1970; 227:187–189. [PubMed: 5428413]

Baker FC, Tsai LW, Reuter CC, Schooley DA. In vivo fluctuations of JH, JH acid, and ecdysteroid titer, and JH esterase activity during development of the fifth stadium *Manduca sexta*. Insect Biochem. 1987; 17:989–996.

Bayer CA, von Kalm L, Fristrom JW. Relationships between protein isoforms and genetic functions demonstrate functional redundancy at the BroadComplex during *Drosophila* metamorphosis. Dev Biol. 1997; 187:267–282. [PubMed: 9242423]

Beckstead RB, Lam G, Thummel CS. The genomic response to 20-hydroxyecdysone at the onset of *Drosophila* metamorphosis. Genome Biol. 2005; 6:R99. [PubMed: 16356271]

Beeman RW, Staurt JJ. A gene for lindane+cyclodeine resistance in the red flour beetle (Coleoptera: Tenebrionidae). J Econ Entomol. 1990; 83:1745–1751.

Belyaeva ES, Aizenon M, Kiss I, Gorelova T, Pak S, Umbetova G, Kramers P, Zhimulev IF. New mutants *Drosophila*. Inform Serv. 1982; 58:184–190.

Emery IF, Bedian V, Guild GM. Differential expression of broad-complex transcription factors may forecast tissue-specific developmental fates during *Drosophila* metamorphosis. Development. 1994; 120:3275–3287. [PubMed: 7720567]

Erezyilmaz DF, Riddiford LM, Truman JW. The pupal specifier Broad directs progressive morphogenesis in a direct-developing insect. Proc Natl Acad Sci USA. 2006; 103:6925–6930. [PubMed: 16641104]

Feng QL, Ladd TR, Tomkins BL, Sundaram M, Sohi SS, Retnakaran A, Davey KG, Palli SR. Spruce budworm (*Choristoneura fumiferana*) juvenile hormone esterase: hormonal regulation, developmental expression and cDNA cloning. Mol Cell Endocrinol. 1999; 148:95–108. [PubMed: 10221775]

Fristrom DK, Fekete E, Fristrom JW. Imaginal disc in a nonpupariating lethal mutant in *Drosophila melanogaster*. Wilhelm Roux's Arch Dev Biol. 1981; 190:11–21.

Gelman DB, Blackburn MB, Hu JS. Timing and ecdysteroid regulation of the molt in last instar greenhouse whiteflies (*Trialeurodes vaporariorum*). J Insect Physiol. 2002; 48:63–73. [PubMed: 12770133]

Gelman DB, Gerling D, Blackburn MB, Hu JS. Hostparasite interactions between whiteflies and their parasitoids. Arch Insect Biochem Physiol. 2005; 60:209–222. [PubMed: 16304614]

Guay PS, Guild GM. The ecdysone-induced puffing cascade in *Drosophila* salivary glands: a broad-complex early gene regulates intermolt and lategene transcriptions. Genetics. 1991; 129:169–175. [PubMed: 1936956]

Haliscak JP, Beeman RW. Status of malathion resistance in five genera of beetles infesting farm-stored corn, wheat and oats in the United States. J Econ Entomol. 1983; 76:717–722.

Karim FD, Guild GM, Thummel CS. The *Drosophila* broad complex plays a key role in controlling ecdysone-regulated gene expression at the onset of metamorphosis. Development. 1993; 118:977–988. [PubMed: 8076529]

Kethidi DR, Xi Z, Palli SR. Developmental and hormonal regulation of juvenile hormone esterase gene in *Drosophila melanogaster*. J Insect Physiol. 2005; 51:393–400. [PubMed: 15890182]

Kingan TG, Adams ME. Ecdysteroids regulate secretory competence in Inka cells. J Exp Biol. 2000; 203:3011–3018. [PubMed: 10976037]

Kingan TG. A competitive enzyme-linked immunosorbent assay: applications in the assay of peptides, steroids, and cyclic nucleotides. Anal Biochem. 1989; 183:283–289. [PubMed: 2560350]

Kiss I, Szabad J, Major J. Genetic and developmental analysis of puparium formation in *Drosophila*. Mol Gen Genet. 1978; 164:77–83.

Kiss I, Beaton AH, Tardiff J, Fristrom D, Fristrom JW. Interactions and developmental effects of mutations in the Broad-complex of *Drosophila melanogaster*. Genetics. 1988; 118:247–259. [PubMed: 3129334]

Kiss I, Bencze G, Fodor G, Szabad J, Fristrom JW. Prepupal larval mosaics in *Drosophila melanogaster*. Nature. 1976; 262:136–138. [PubMed: 819843]

Margam VM, Gelman DB, Palli SR. Ecdysteroid titers and developmental expression of ecdysteroid-regulated genes during metamorphosis of the yellow fever mosquito, *Aedes aegypti* (Diptera:Culicidae). J Insect Physiol. 2006; 52:558–568. [PubMed: 16580015]

Nagel RH. Metathetely in larvae of the confused flour beetle (*Tribolium confusum* Duvai). Ann Entomol Soc Am. 1934; 27:425–428.

Nation JL. A new method using hexamethyldisilazane for preparation of soft insect tissues for scanning electron microscopy. Stain Tech. 1983; 58:347–351.

Nijhout, HF. Insect Hormones. Princeton University Press; Princeton, NJ: 1994.

Parthasarathy R, Palli SR. Stage- and cell-specific expression of ecdysone receptors and ecdysone-induced transcription factors during midgut remodeling in the yellow fever mosquito, *Aedes aegypti*. J Insect Physiol. 2007; 53:216–229. [PubMed: 17074360]

Postlethwait JH. Juvenile hormone and the adult development of *Drosophila*. Biol Bull. 1974:147.

Quennedey A, Quennedey B. Morphogenesis of the wing anlagen in the mealworm beetle *Tenebrio molitor* during the last larval instar. Tissue Cell. 1990; 22:721–740. [PubMed: 18620327]

Restifo LL, White K. Mutations in a steroid hormone regulated gene disrupt the metamorphosis of the central nervous system in *Drosophila*. Dev Biol. 1991; 148:174–194. [PubMed: 1936557]

Restifo LL, White K. Mutations in a steroid hormone regulated gene disrupt the metamorphosis of internal tissues in *Drosophila* salivary glands, muscles, and gut. Wilhelm Roux's Arch Dev Biol. 1992; 201:221–234.

Restifo LL, Wilson TG. A juvenile hormone agonist reveals distinct developmental pathways mediated by ecdysone-inducible broad complex transcription factors. Dev Genet. 1998; 22:141–159. [PubMed: 9581286]

Reza AMS, Kanamori Y, Shinoda T, Shimura S, Mita K, Nakahara Y, Kiuchi M, Kamimura M. Hormonal control of a metamorphosis-specific transcriptional factor broad-complex in silkworm. Comp Biochem Physiol. 2004; 139:753–761.

Riddiford LM. Hormonal control of insect epidermal cell commitment in vitro. Nature. 1976; 259:115–117. [PubMed: 1246347]

Riddiford LM. Ecdysone-induced change in cellular commitment of the epidermis of the tobacco hornworm, *Manduca sexta* at the initiation of metamorphosis. Gen Comp Endocrinol. 1978; 34:438–446. [PubMed: 648872]

Riddiford LM. Hormone receptors and the regulation of insect metamorphosis. Receptor. 1993; 3:203–209. [PubMed: 8167571]

Riddiford LM. Cellular and molecular actions of juvenile hormone. I General considerations and premetamorphic actions. Adv Insect Physiol. 1994; 24:213–274.

Riddiford, LM. Molecular aspects of juvenile hormone action in insect metamorphosis. In: Gilbert, LI.; Tata, JR.; Atkinson, BG., editors. Metamorphosis: Postembryonic Reprogramming of Gene Expression in Amphibian and Insect Cells. Academic Press; San Diego: 1996. p. 223-251.

Riddiford LM, Ashburner M. Effects of juvenile hormone mimics on larval development and metamorphosis of *Drosophila melanogaster*. Gen Comp Endocrinol. 1991; 82:172–183. [PubMed: 1906823]

Russell, S.; Ashburner, M. Ecdysone-regulated chromosome puffing *Drosophila melanogaster*. In: Gilbert, LI.; Tata, JR.; Atkinson, BG., editors. Metamorphosis: Post-embryonic Reprogramming of Gene Expression in Amphibian and Insect Cells. Academic Press; San Diego: 1996. p. 109-144.

Svacha P. What are and what are not imaginal discs:reevaluation of some basic concepts (Insects, Holometabola). Dev Biol. 1992; 154:101–117. [PubMed: 1426619]

Thummel CS. Flies on steroids-*Drosophila* metamorphosis and the mechanisms of steroid hormone action. Trends Genet. 1996; 12:306–310. [PubMed: 8783940]

Tower WL. The origin and development of the wings of Coleoptera. Zool Jahresber. 1903; 17:515–572.

Truman JW, Riddiford LM. Endocrine insights into the evolution of metamorphosis in insects. Annu Rev Entomol. 2002; 47:467–500. [PubMed: 11729082]

Uhlirova M, Foy BD, Beaty BJ, Olson KE, Riddiford LM, Jindra M. Use of Sindbis virus-mediated RNA interference to demonstrate a conserved role of broad-complex in insect metamorphosis. Proc Natl Acad Sci USA. 2003; 100:15607–15612. [PubMed: 14668449]

Zhou B, Hiruma K, Shinoda T, Riddiford LM. Juvenile hormone prevents ecdysteroid-induced expression of broader complex RNAs in the epidermis of the tobacco hornworm *Manduca sexta*. Dev Biol. 1998; 203:233–244. [PubMed: 9808776]

Zhou B, Riddiford LM. Hormonal regulation and patterning of the broad-complex in the epidermis and wing discs of the tobacco hornworm *Manduca sexta*. Dev Biol. 2001; 231:125–137. [PubMed: 11180957]

Zhou X, Riddiford LM. Broad specifies pupal development and mediates the 'status quo' action of juvenile hormone on the pupal–adult transformation in *Drosophila* and *Manduca*. Development. 2002; 129:2259–2269. [PubMed: 11959833]

Zollman S, Godt D, Prive GG, Coudere JL, Laski FA. The BTB domain, found primarily in zinc finger proteins, defines an evolutionary conserved family that includes several developmentally regulated genes in *Drosophila*. Proc Natl Acad Sci USA. 1994; 91:10717–10721. [PubMed: 7938017]

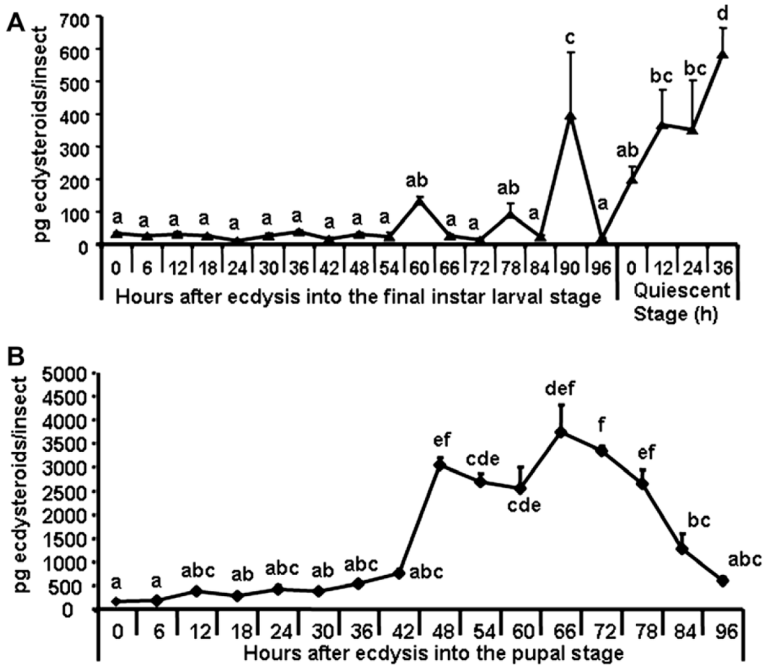

Fig. 1.

Estimation of ecdysteroid levels in the final instar larval (A) and pupal (B) stages of *T. castaneum*. Insects were staged every 6 h during the final instar larval stage (0–96), every 12 h during the quiescent stage (0–36), every 6 h during the pupal stage (0–96). Ecdysteroid levels were estimated using enzyme immunoassay as previously described (Kingan and Adams, 2000; Gelman et al., 2002). Each time point represents mean ± SE of 10 individual insects. Each time point was replicated three times. Means with the same letter are not significantly different ($\alpha \leq 0.05$; ANOVA).

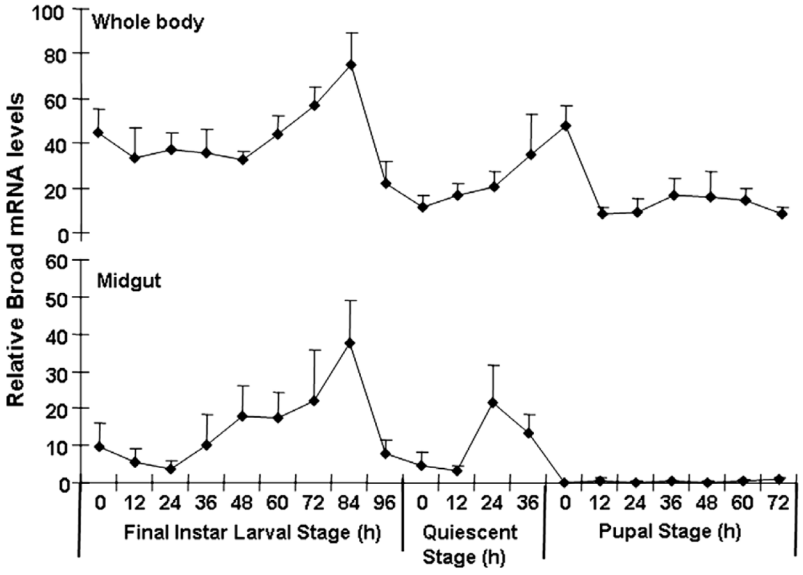

Fig. 2.

mRNA levels of Tcbr in the whole body and the midgut of *T. castaneum* determined by quantitative reverse-transcriptase real-time PCR (qRT-PCR). Samples were collected at 12 h interval during the final instar larval and pupal stages. Total RNA was extracted from pools of three larvae for each treatment. The *Y*-axis denotes expression levels normalized using the rp49 levels as an internal control. Mean ± SE of two independent experiments with three replications each are shown.

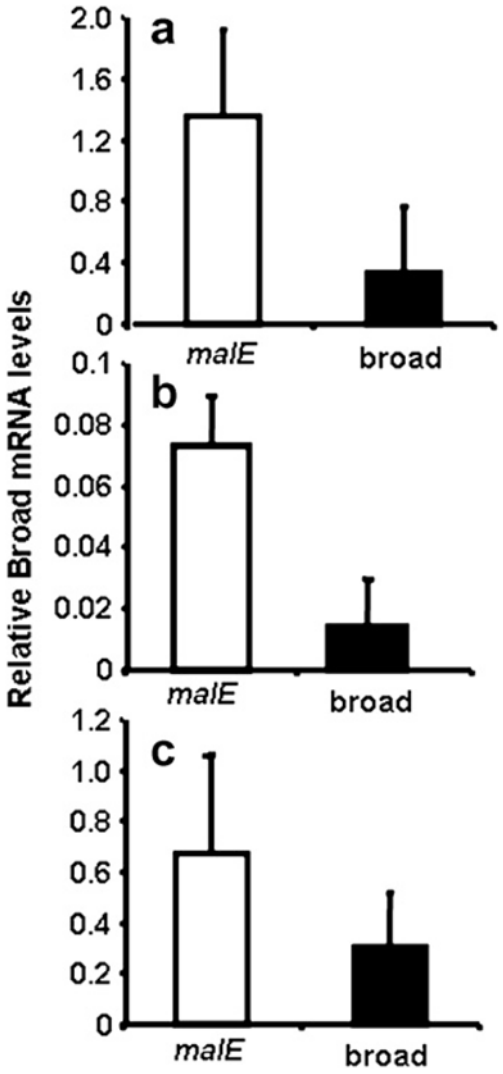

Fig. 3.

mRNA levels of Tcbr in dsRNA injected and control insects. dsRNA injections were done during penultimate larval stage (a), final instar larval stage [24 h (b) and 72 h AEFL (c)]. The insects were sampled at 4–5 days after injection. See text for details. Total RNA was extracted from individual three larvae for each treatment. cDNAs prepared from the RNA were used in qRT-PCR. The relative expression levels of Tcbr mRNA were determined using the levels of rp49 as an internal control. Mean ± SE of three independent experiments are shown.

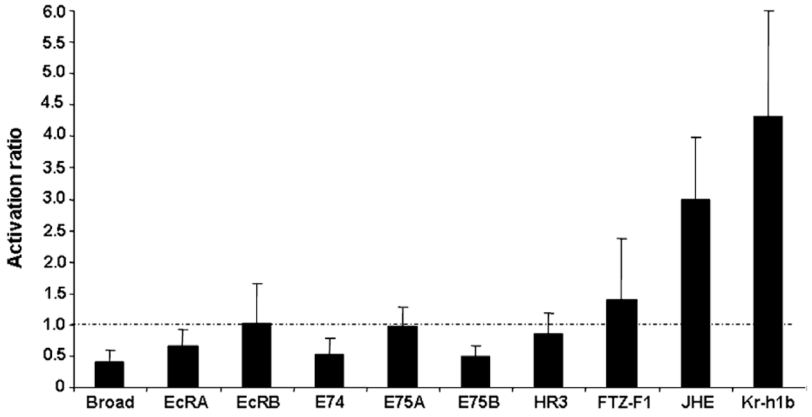

Fig. 4.

The activation ratio of mRNA levels of 20E- and JH-response genes in insects injected with Tcbr dsRNA. The mRNA levels of 20E-response genes (Broad, EcRA, EcRB, HR3, FTZ-F1, E74, E75A and E75B) and JH-response genes (JHE and Kr-h1b) were determined in insects injected with Tcbr dsRNA using qRT-PCR. Tcbr dsRNA injected at 24 h AEFL and total RNA was extracted from pools of three larvae for each treatment at 4 days after injection. cDNAs prepared from the RNA were used for qRT-PCR analysis. The mRNA levels were normalized using the levels of rp49 as an internal control. The expression levels of each gene in the corresponding control insects injected with *malE* dsRNA was set as 1 (dashed line). Mean ± SE for three independent experiments are shown.

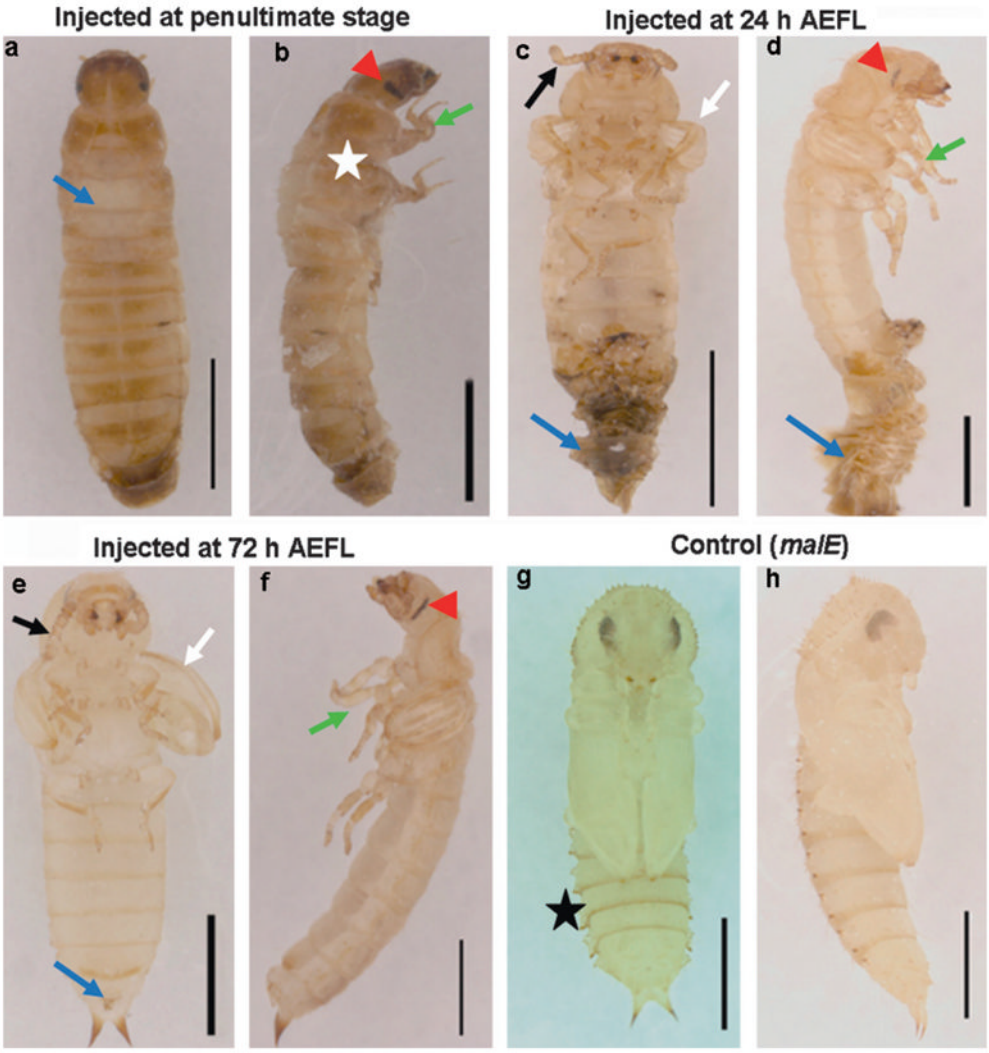

Fig. 5.

Phenotypes of knock-down of Tcbr. Tcbr or *malE* dsRNA (control) was injected into penultimate larval stage (a and b) or at 24 h (c and d) or at 72 h (e and f) after ecdysis into the final instar larval stage and the corresponding phenotypes are shown in comparison with control (g and h)). (a) The dorsal view, (c, e and g) the ventral view and (b, d, f and h) the lateral view of Tcbr RNAi and *malE* RNAi (control) insects. Injections were given within 24 h of penultimate larval stage and 24 and 72 h of last instar larval stage. (a) Split in the dorsal thoracic region (blue arrow). (b) Wing pads (white star), compound eyes (red arrow-head) and differentiated legs (green arrow). (c and d) The exuviae remained attached to the body (blue arrow) when injections are done at 24 h AEFL. Irrespective of time of injection, note the development of antennae (c and e, black arrows), wings (c and e, white arrows), legs (d and f, green arrow) and compound eyes (d and f, red arrowhead) at different differentiating states. Note the absence of gin-traps in Tcbr dsRNA injected insects (c and e) but present in the control pupal abdomen (g, black star). Scale bar: 1 mm.

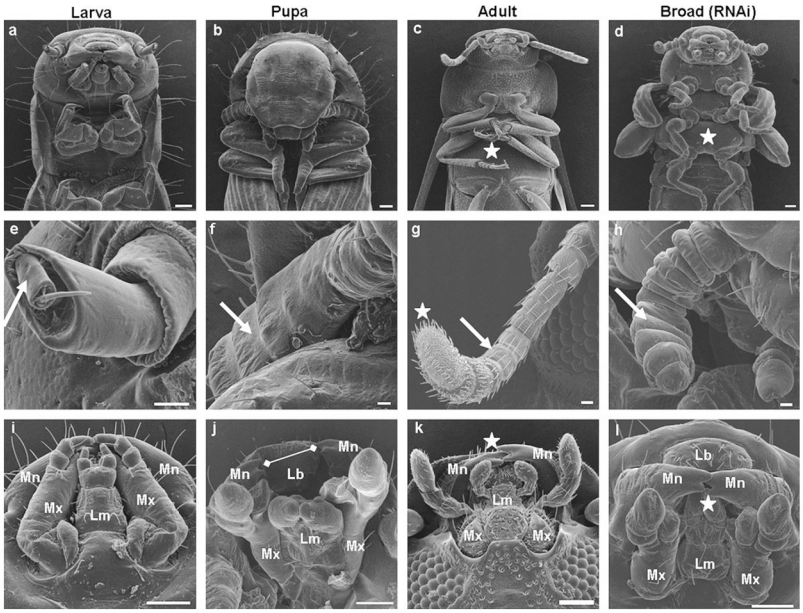

Fig. 6.

Knock-down in Tcbr expression results in expression of larval, pupal and adult characters in the same insects. Tcbr dsRNA was injected into the final instar larvae (at 24 h) and SEM images of various organs are compared with wild-type larval/pupal/adult counterparts (a–l). (a–d) Head and thoracic region, (e–h) antennae and (i–l) mouthparts. All panels show ventral side of insects orienting head to the top and abdomen to the bottom. (a–d) well developed thoracic sternal plates (white star). (e–h) Flagellar segments of the antenna (white arrow) and hygroscopic receptors wherever present (white star). (i–l) Mandibles (Mn), labrum (Lb), maxilla (Mx) and labium (Lm); absence of gaps between incisors observed in the pupal mandibles (j, white arrow line); interlocking of mandibles (k and l, white star). Scale bar: (a–d) 100 μm; (e–h) 20 μm; (i–l) 100 μm.

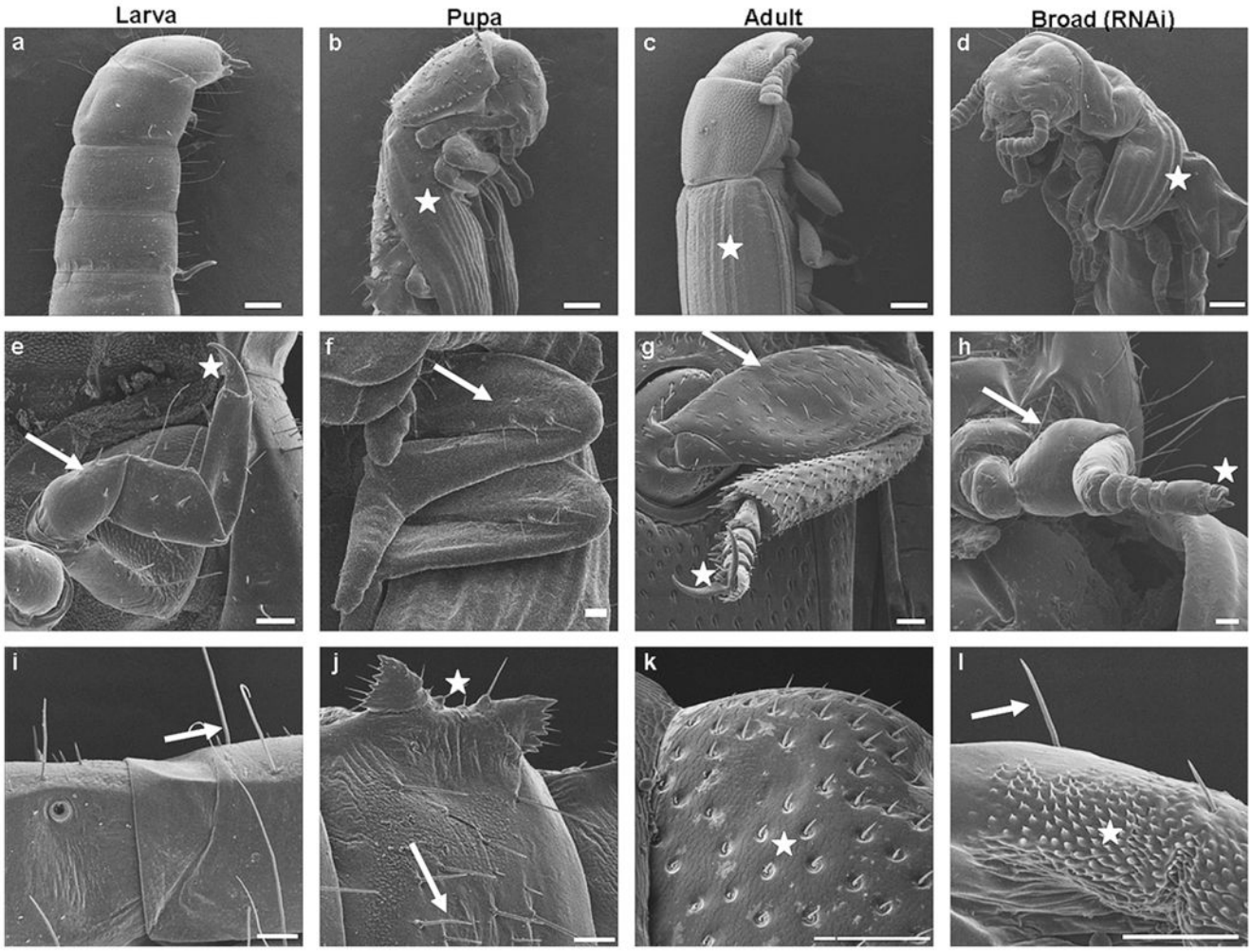

Fig. 7.

Knock-down in Tcbr expression affects cuticular structures as well as differentiation of legs and wings. Tcbr dsRNA was injected into the final instar larvae (at 24 h) Panels show SEM images of wings (a–d), legs (g–h) and abdominal cuticle (i–l) in insects injected with Tcbr dsRNA and uninjected larva, pupa and adults. (a–d) The lateral view and (e–l) the ventral view of insects. (b–d)Wings are denoted by white star. (e–h) Femur segment (white arrow); claw (white star). (i–l) Abdominal cuticular structures; long setae (i and l, white arrow); gin-traps (j, white star); short setae (j, white arrow); sensory bristles (k and l, white star). See text or Table 3 for description. Scale bar: (a–d) 200 μm; (e–h) 50 μm; (i–l) 50 μm.

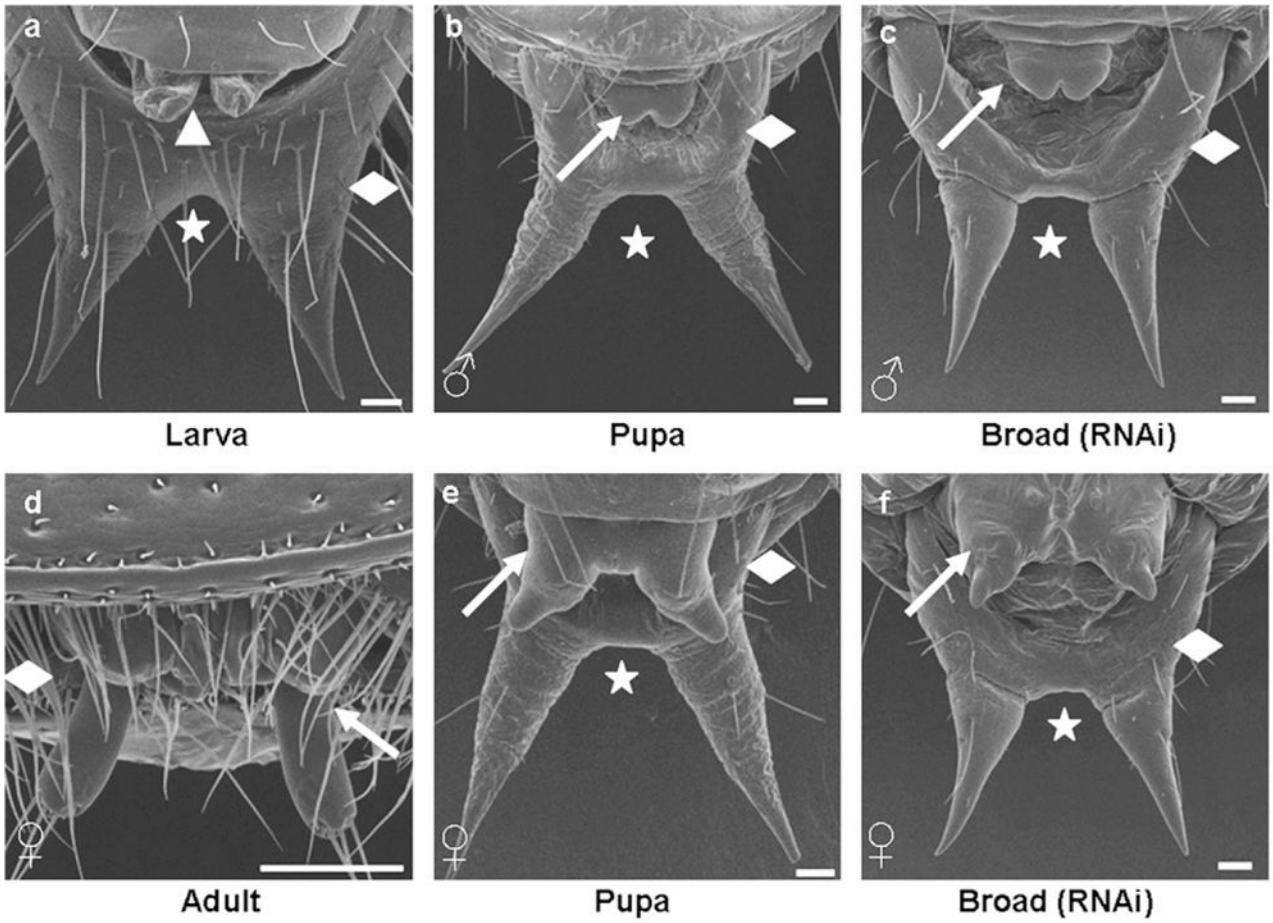

Fig. 8.

Knock-down in Tcbr expression does not block development of genital papillae and modification of urogomphi. Tcbr dsRNA was injected into the final instar larvae (at 24 h). Panels show SEM images of ventral side of abdominal distal segments of wild-type larva (a), male pupa (b), female pupa (e), female adult (d) and Tcbr RNAi male (c) and female insects (f). Male genital papillae (b and c, white arrow) and female genital papillae (e and f, white arrow) are shown. (a) Included to show the pair of pygopods (white arrow-head) present only in larval stages. Wild-type adult male is not shown as the genital papillae are concealed. (a–f) The distal abdominal segment (white diamond) and urogomphi (white star). See text or Table 3 for description. Scale bar: 50 μm.

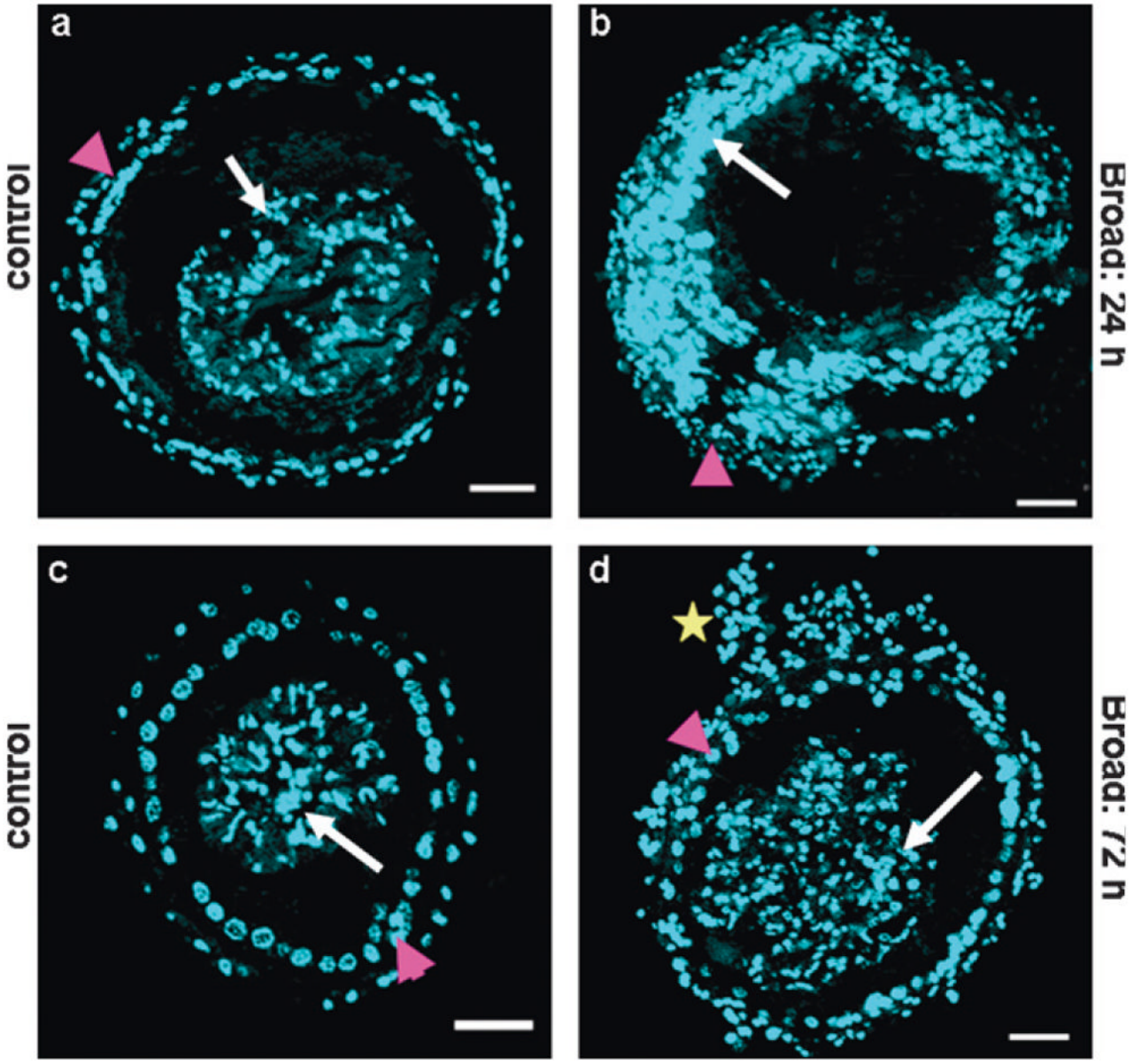

Fig. 9.

Knock-down in Tcbr expression affects midgut remodeling. Tcbr dsRNA or *malE* (control) dsRNA was injected at 24 and 72 h AEFL. Cross-sections (CS, 10 μm thick) of midguts dissected from insects dissected 5 days after dsRNA injection and nuclear stained with DAPI are shown (a–d). (a and b) The comparison of CS of midgut dissected from insects injected with Tcbr dsRNA at 24 h AEFL. (c and d) Midguts dissected from insects injected with Tcbr dsRNA at 72 h AEFL. The pupal/adult cells (pink arrow head) and larval cells (white arrow) are shown (a–d). Note the formation of crypt-like evagination (d, yellow star) in the midgut dissected from larvae injected with Tcbr dsRNA at 72 h AEFL. Scale bar: 50 μm.

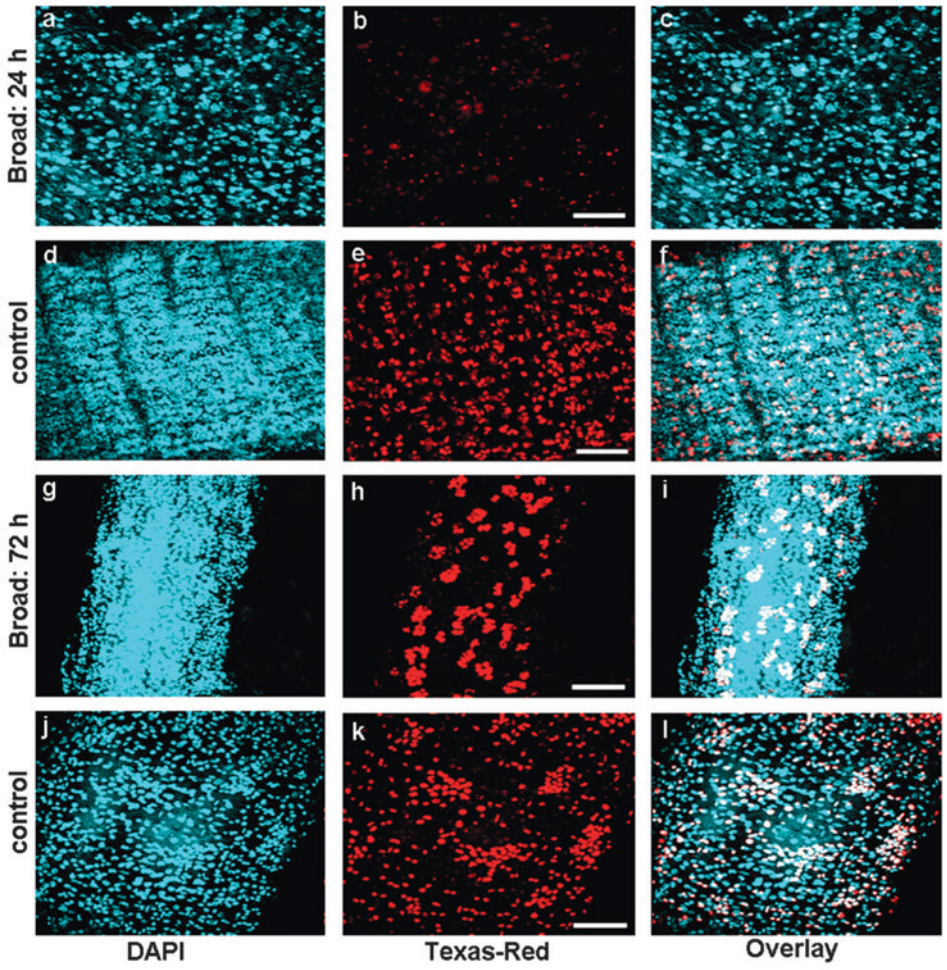

Fig. 10.

Effect of Tcbr RNAi on the cell proliferation of midgut. Cell proliferation assay was performed using BrdU. BrdU was administered in insects injected with Tcbr or *malE* (control) dsRNA after four days of injection. The detection of proliferating cells was performed using anti-BrdU primary antibody and Texas-Red conjugated secondary antibody. Panels show nuclear staining by DAPI (a, d, g and j), proliferating cells staining by BrdU (b, e, h and k) and overlay of both (c, f, i and l). Injection of Tcbr dsRNA at 24 AEFL blocked cell proliferation in midgut and only a few BrdU positive cells were observed (b) when compared to its control (e). Injection of Tcbr dsRNA at 72 h AEFL showed midgut in advanced state of proliferation with evagination of crypts (h) when compared to its control (k). Only proliferating imaginal cells were detected by BrdU (white in overlay images); larval or differentiated pupal cells remain unstained (blue in overlay images). Controls include insects not injected with BrdU (not shown). Scale bar: 20 μm.

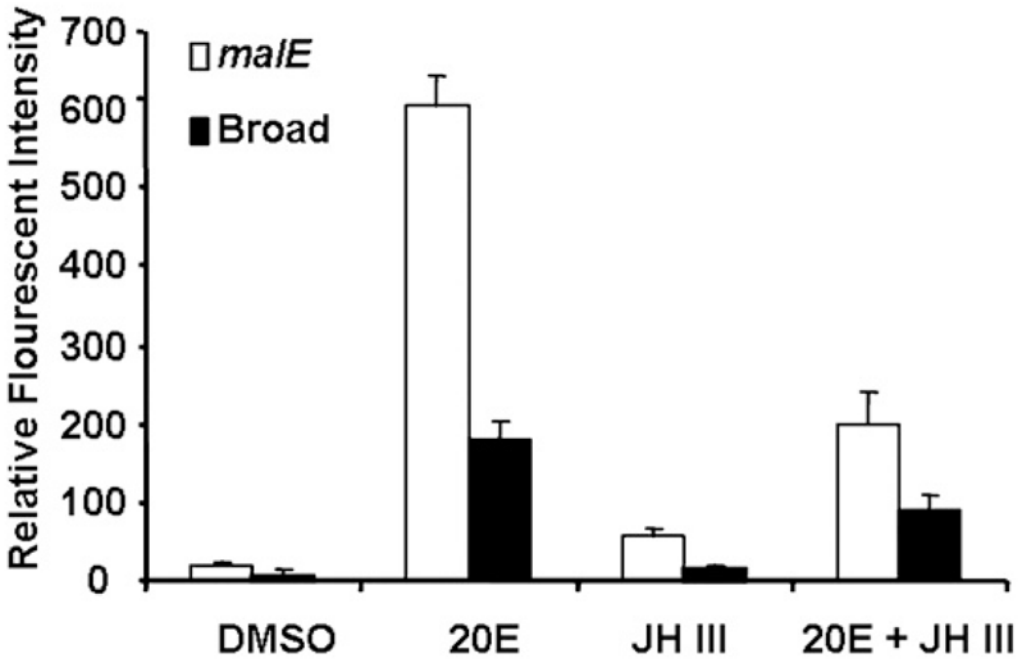

Fig. 11.

Relative florescence intensity (RFI) of proliferating cells in *in vitro* cultured midguts dissected from insects injected with Tcbr or *malE* dsRNA exposed to DMSO, 20E, JH III or 20E + JH III and quantified using BrdU labeling. RFI was measured using Olympus Flouview software version 1.5. Squares of constant area (6662mm^2) and length (26 mm) were drawn on composite *Z*-stack images. The average intensity in the marked area against the background was measured using the software. All other parameters (PMT, Gain, Offset, zoom) were the same for each image documented. Mean ± SE of three independent experiments (n = 15) are shown.

Table 1

List of primers used in qRT-PCR and RNAi

Genes	Forward: 5′–3′	Reverse: 5′–3′
For qRT-PCR		
EcRA[a]	TACAGCCCCAACGGAAAGAT	GATACACCGCGTTCTTCGTT
EcRB	GACCTGGAGTTCTGGGACCT	CTTGGCTAGATGGTGGTTGC
Tcbr	CACAACACTTCTGTCTGCGGTG	CACAGGGTGTTTGCAAGGAG
HR3	CCGTGCAAAGTATGTGG	GTCGGCAGTATTGACATC
E74	GCGTCTTCAAGCTGGTG	CAGCCTTTGACCGTCCAC
E75A[b]	GAAATCGCGTCCAAGTG	GAAGGAAGTTCAATGGC
E75B[b]	GAAATCGCGTCCAAGTG	CGGGGATGGAGCTGGAGG
FTZ-F1	TGCGAGGAATCACAAACAAG	TGCAGTGCTTGTGGTAGAGG
JHE	ACTTTACGTGGGGTGTGAGC	TTGATGAGGATCGGGATTTC
Kr-h1B	TGTGACGTTTGCTCGAAGAC	GCACGAGTAGGGCTTTTCAC
Rp49	TGACCGTTATGGCAAACTCA	TAGCATGTGCTTCGTTTTGG
For dsRNA		
Tcbr-common	TCTACTCCTTGCAAACACCCTG	GGTGAGCCCGCTGACCCGGAGC

[a]Forward primer from EcRA specific exon and reverse primer from common exon were used to monitor EcRA mRNA levels.

[b]Common forward primer and specific reverse primers were used to monitor E75A and E75B mRNA levels.

Table 2

Effect of injection of dsRNA for Tcbr on metamorphosis

Stage of larvae injected	dsRNA	No. larvae injected	Normal pupae	Larval–pupal–adult intermediates	Normal adults
Penultimate	Tcbr	32	0	32	0
	malE	35	35	0	32
24 h-old final instar	Tcbr	30[a]	0	28	0
	malE	33	33	0	28
72 h-old final instar	Tcbr	30[a]	0	25	0
	malE	30	28	0	28

[a]A few larvae died on first and second day after injection most likely due to injection injury.

Table 3

Morphological characters of Broad RNAi insects in comparison with wild-type larva/pupa/adult

S. No.	Organs	Characters				Comments[a]
		Larva	Pupa	Adult	Broad RNAi	
1.	Thoracic sternal plates	Normal	Normal; concealed	Well developed; sclerotized	Well developed; not sclerotized	Resemble adults except for sclerotization
2.	Antennae	Contains scape and pedicel; flagellum not developed	Flagellar segments developing, 5–6 No.	Flagellar segments developed, 10–11 No.; hygroscopic receptors present	Flagellar segments 10–11 No.; hygroscopic receptors absent	Resemble adults except for hygroscopic receptors
3.	Mouthparts	Labrum concealed; mandible prominent; maxillary and labial palpi short	Labrum prominent; mandible separated; palpi developing	Labrum concealed; mandible interlocked; palpi well developed	Labrum prominent; mandible interlocked; palpi developing	Pupal–adult intermediate
4.	Forewings	Absent	Developed; not sclerotized; cover 2/3 of abdomen	Well developed; well sclerotized; cover entire abdomen	Short; medium sclerotization; do not cover abdomen	Unique character
5.	Legs	Segments not distinct; single claw	Concealed in pupal cuticle	Sclerotized; segments distinct; tarsi differentiated; pair of claw; spurs present	Medium sclerotized; short; bulbous femur; segments distinct; tarsi differentiated; pair of claw; spurs absent	Resemble adult except for size and differentiation of segments
6.	Abdominal cuticular structures	Long setae	Short setae; gin-traps laterally	Sensory bristles	Patches of sensory bristles and long setae; gin-traps absent	Mosaic of larval and adult structures
7.	Distal abdominal segment (both sexes)	Distinct	Contracted	Telescopic	Distinct	Resemble larva
8.	Genital papillae (both sexes)	Absent; pygopods present	Well developed in both sexes	Well developed in female; male concealed	Well developed in male; incomplete in female	Resemble pupa except for size of female genital papillae
9.	Urogomphi (both sexes)	Sclerotized; fused at top	Not sclerotized; tubular; separated by median at top	Absent	Sclerotized; tubular; separated by median at top	Larval–pupal intermediate

Characters are scored based on the light microscope and SEM images (Figs. 5–8).

[a]Comparisons are made based on the similarities of structures of Broad RNAi insects with wild-type larva/pupa/adult counterparts.